JOURNAL OF MATERIALS SCIENCE 31 (1996) 6223–6228

SiC–TiC and SiC–TiB_2 composites densified by liquid-phase sintering

KYEONG-SIK CHO, YOUNG-WOOK KIM*, HEON-JIN CHOI, JUNE-GUNN LEE
Division of Ceramics, Korea Institute of Science and Technology, P.O. Box 131, Cheongryang, Seoul 130–650, Korea
**Department of Materials Science Engineering, Seoul City University, 90 Jeonnong-Dong, Dongdaemoon-Ku, Seoul 130-743, Korea*

Particle-reinforced SiC composites with the addition of TiC or TiB_2 were fabricated at 1850 °C by hot-pressing. Densification was accomplished by utilizing a liquid phase formed with added Al_2O_3, Y_2O_3, and surface SiO_2 on SiC. Their mechanical and electrical properties were measured as a function of TiC or TiB_2 content. Adding TiC or TiB_2 to the SiC matrix increased the toughness, and decreased the strength and electrical resistivity. The fracture toughnesses of SiC–50 wt% TiC and SiC–50 wt% TiB_2 composites were approximately 60% and 50%, respectively, higher than that of monolithic SiC ceramics. Microstructural analysis showed that the toughening was due to crack deflection, with some possible contribution from microcracking in the vicinity of TiC or TiB_2 particles.

1. Introduction

SiC ceramics are promising candidates for applications as high-temperature structural materials because of their excellent creep resistance and oxidation behaviour [1–3]. However, low fracture toughness and difficulties in machining due to chipping, which arises from their brittleness and high hardness, limit their wide application under stress or impact [4, 5]. Recently, *in situ* toughening using $\beta \rightarrow \alpha$ phase transformation of SiC was reported as one of the promising methods to increase the toughness [6, 7]. Particle reinforcement is also a promising method to overcome the brittleness. Dispersing boride and carbide particles such as TiB_2 [8] and TiC [9] have already been investigated. These materials have higher elastic modulus, higher hardness, higher thermal expansion coefficient, and lower electrical resistivity than SiC. The higher thermal expansion of the reinforcing particles causes radial tensile stresses and tangential compressive stresses in the SiC matrix due to the thermal expansion mismatch [10]. The stresses make the crack deflection around the reinforcing particles easy, resulting in the increased fracture toughness. Also, lower electrical resistivity of the reinforcing particles makes electrical discharge machining (EDM) of the material possible. EDM is especially effective for machining of complicated shapes, which is impossible or costly by other conventional methods [11–14].

There are no difficulties in fabricating dense SiC composites, such as SiC–TiC and SiC–TiB_2 composites, by hot-pressing at temperatures higher than 2000 °C [8, 9], although low-temperature hot-pressing or pressureless sintering is more economical.

In this study, particle-reinforced SiC composites, such as TiC and TiB_2 were fabricated by hot-pressing at 1850 °C which is relatively low for the sintering of SiC–TiC and SiC–TiB_2 composites. Their mechanical and electrical properties were determined as a function of the content of reinforcing particles.

2. Experimental procedure

Mixtures of β-SiC (Betarundum, Ultrafine, Ibiden Co., Ltd, Nagoya, Japan), a titanium compound such as TiC (Grade c.a.s, H.C. Starck, Berlin, Germany) and TiB_2 (Grade F, H.C. Starck, Berlin, Germany), Al_2O_3 (AKP-30, Sumitomo Chemicals, Tokyo, Japan), and Y_2O_3 (Grade Fine, H.C. Starck, Berlin, Germany) were milled for 24 h using a polyethylene jar and SiC balls in ethanol. The mixed slurries were then dried, subsequently sieved through a 60 mesh screen, and hot-pressed at 1850 °C for 1 h with 25 MPa applied pressure in an argon atmosphere. The batch compositions are summarized in Table I.

Densities were evaluated using Archimedes' method. Theoretical densities were calculated assuming a rule of mixtures. X-ray diffractometry (XRD) was used to determine the crystalline phases. The microstructures of hot-pressed samples were observed by optical microscopy and scanning electron microscopy (SEM). The hot-pressed materials were machined into 3 mm × 4 mm × 25 mm bars with an 800 grit diamond wheel for flexural testing. Four-point flexural strength was measured at room temperature with outer and inner spans of 20 and 8 mm, respectively. The fracture toughness was determined by using a Vickers' indentor

0022–2461

TABLE I Properties of monolithic SiC, SiC–TiC and SiC–TiB_2 composites

Specimen designation	Composition wt %					Density		Crystalline phase		Electrical resistivity at 25 °C (Ω cm)
	SiC	TiC	TiB_2	Al_2O_3	Y_2O_3	Bulk density (g cm^{-3})	Relative density (%)	Major phase	Minor phase	
SC	90	–	–	7	3	3.277	99.42	β-SiC	YAG[a], α-Al_2O_3	0.82
SCTC1	60	30	–	7	3	3.651	99.03	β-SiC, TiC	YAG, α-Al_2O_3	2.32×10^{-2}
SCTC2	40	50	–	7	3	4.000	99.90	β-SiC, TiC	YAG, α-Al_2O_3	3.65×10^{-4}
SCTC3	20	70	–	7	3	4.357	99.44	β-SiC, TiC	YAG, α-Al_2O_3	1.08×10^{-4}
SCTB1	60	–	30	7	3	3.519	97.42	β-SiC, TiB_2	α-Al_2O_3	1.91×10^{-3}
SCTB2	40	–	50	7	3	3.748	97.15	β-SiC, TiB_2	α-Al_2O_3	4.38×10^{-5}
SCTB3	20	–	70	7	3	4.071	98.29	β-SiC, TiB_2	α-Al_2O_3	1.43×10^{-5}

[a] $Al_5Y_3O_{12}$ (Yttrium aluminium garnet).

with a load of 196 N [15]. Electrical resistivity was measured using the four-point probe method.

3. Results and discussion

Table I shows the results of sintered densities and crystalline phases of hot-pressed samples. The relative densities of all samples were higher than 96% theoretical. This indicates that SiC–TiC and SiC–TiB_2 composites with Al_2O_3 and Y_2O_3 as sintering additives can be densified at a temperature as low as 1850 °C. The sintering temperature is about 150–300 °C lower than those used for composites without or with other sintering additives in earlier works [8–10]. Al_2O_3 and Y_2O_3 additives in the sintering of SiC are known to form liquid phase with the surface SiO_2 of SiC and to promote densification through liquid-phase sintering [16, 17]. Polycrystalline TiC and TiB_2 (doped with 2 wt % carbon) can easily be fabricated to over 99% theoretical densities by hot-pressing at 1700–1850 °C with 35–70 MPa applied pressure without or with sintering additives [18, 19]. Such hot-pressing behaviour of TiC and TiB_2, and the beneficial function of Al_2O_3 and Y_2O_3 in the densification of SiC resulted in the successful densification of the SiC–TiC and SiC–TiB_2 composites in the present work. Analysis by XRD of the monolithic SiC, SiC–TiC and SiC–TiB_2 composites revealed β-SiC, TiC and TiB_2 as major phases and $Al_5Y_3O_{12}$ (ytrrium–aluminium garnet, YAG) and/or α-Al_2O_3 as minor phases.

Fig. 1 shows optical micrographs of polished surfaces of hot-pressed samples with TiC and TiB_2 content of 0–70 wt %. The bright phase is TiC or TiB_2 and the grey matrix is SiC. As shown, the composites are two-phase particulate composites consisting of randomly distributed TiC or TiB_2 particles ranging from 1–15 μm in the SiC matrix. Most of dispersed particles are single grains in SiC–30 wt % TiC and SiC–30 wt % TiB_2 composites, but some are clustered of several grains and interconnected with each other in SiC–50 wt % TiC and SiC–50 wt % TiB_2 composites. In SiC–70 wt % TiC and SiC–70 wt % TiB_2 composites, most of the dispersed particles are clustered and interconnected with each other. This may occur because of the greater probability of clustering of TiC or TiB_2 particles as the amount of addition is increased.

The changes in flexural strength and fracture toughness with the weight fraction of reinforcing particles are shown in Fig. 2. As shown, fracture toughness increased with the content of reinforcing particles and showed a maximum at 50 wt % reinforcing particles. The maximum fracture toughnesses of 4.5 and 4.2 MPa $m^{1/2}$ for SiC–50 wt % TiC and SiC–50 wt % TiB_2 composites, respectively, were obtained and these were approximately 60% and 50% higher than that of monolithic SiC (2.7 MPa $m^{1/2}$). The fracture toughness of SiC–70 wt % TiC and SiC–70 wt % TiB_2 composites were lower than those of SiC–50 wt % TiC and SiC–50 wt % TiB_2 composites. This may be due to the transgranular fracture of large TiC and TiB_2 particles (Fig. 3), and the partial loss of composite effect in SiC–70 wt % TiC and SiC–70 wt % TiB_2 composites, where the major phases are TiC and TiB_2. SiC in the TiC or TiB_2 matrix cannot act as reinforcing particles because of the lower elastic modulus and thermal expansion coefficient than TiC or TiB_2. Fig. 2 also shows that flexural strength decreases with the content of reinforcing particles up to 50 wt %, although the fracture toughness increases. The decrease of flexural strength with the content of reinforcing particles will be discussed later.

Fig. 3 shows the fracture surfaces of typical samples. As shown, monolithic SiC consisted of equiaxed grains and fractured mostly in the intergranular mode. In contrast, the fracture mode of SiC–50 wt % TiC and SiC–50 wt % TiB_2 composites was mostly intergranular for smaller grains and transgranular for larger grains, which is believed to be clustering of reinforcing particles.

Fig. 4 shows scanning electron micrographs of cracks induced by a Vickers' indentor. Some crack fronts were deflected and interacted at TiC or TiB_2 particles. The thermal expansion mismatch between matrix and reinforcing particles results in the generation of residual stresses in the particles and surrounding matrix during cooling after hot-pressing. The developed residual stresses, the radial matrix stress, σ_{mr}, and the tangential matrix stress ($\sigma_{m\theta} = -\sigma_{mr}/2$), can be calculated using the following equation based on the hydrostatic stress developed around the particles

$$\sigma_{mr} = \frac{(\alpha_p - \alpha_m)\Delta T}{[(1 + \nu_m)/2E_m] + [(1 - 2\nu_p)/E_p]} \quad (1)$$

where the subscripts p and m refer to the particle and matrix, respectively, α is the thermal expansion coefficient, E is the elastic modulus, ν is the Poisson' ratio, and ΔT is the temperature range over which stresses are not relieved by a diffusive process [20]. The values of the relevant parameters used to perform these calculations are given in Table II. ΔT was assumed to be 1000 °C.

The calculations show that residual radial tensile stresses of ~1500 and ~1900 MPa for SiC–TiC and SiC–TiB_2 composites, respectively, are produced. The high tensile stresses could be relieved by generating microcracking in the vicinity of reinforcing particles. The tangential matrix compressive stresses are ~750 and ~950 MPa for SiC–TiC and SiC–TiB_2 composites, respectively. These stress levels will decrease with decreasing particle radius and with increasing distance from the centre of the particles.

Generally, a crack approaching a particle above or below the crack plane would be deflected towards the radial matrix tensile stress. Observation of the polished surfaces revealed that the cracks were deflected and interacted with the reinforcing particles (Fig. 4b and c). In contrast, monolithic SiC (Fig. 4a)

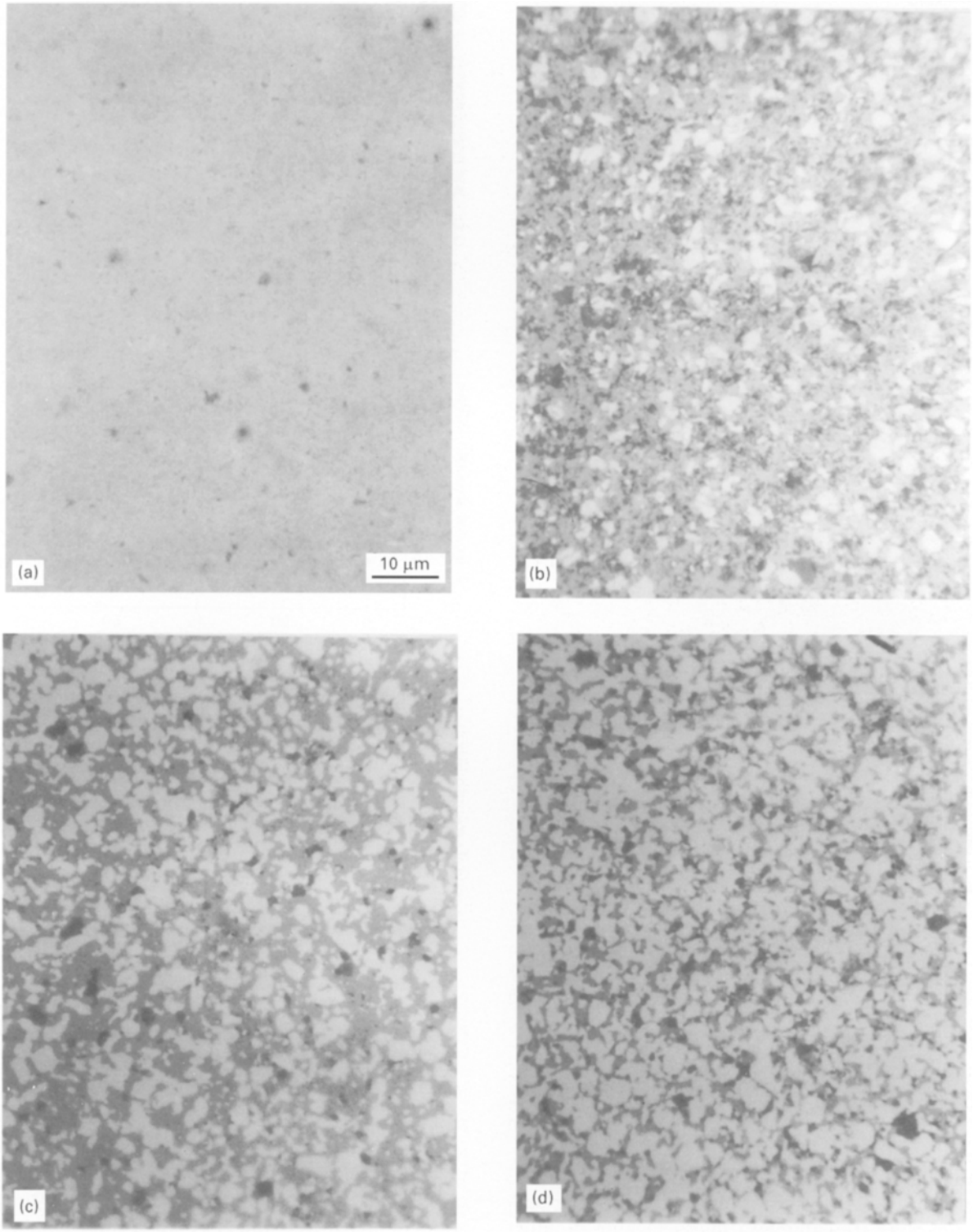

Figure 1 Optical micrographs of polished cross-sections of (a) monolithic SiC, (b) SiC–30 wt % TiC, (c) SiC–50 wt % TiC, (d) SiC–70 wt % TiC, (e) SiC–30 wt % TiB_2, (f) SiC–50 wt % TiB_2, and (g) SiC–70 wt % TiB_2 composites.

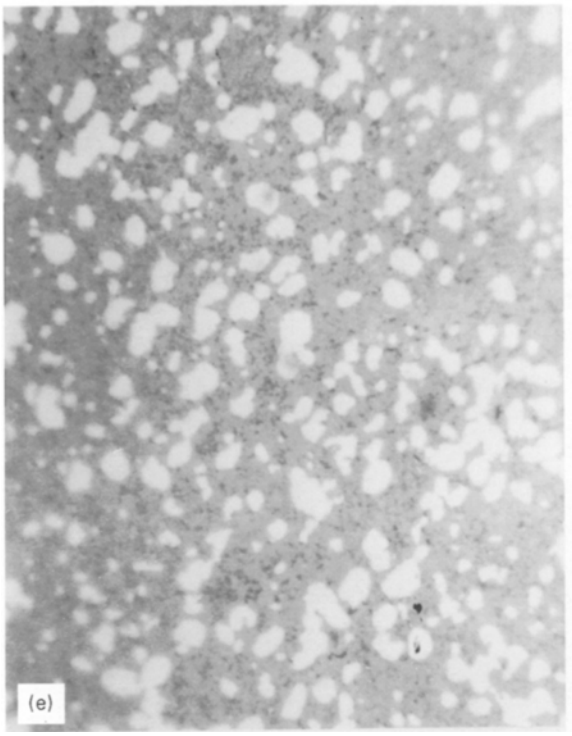

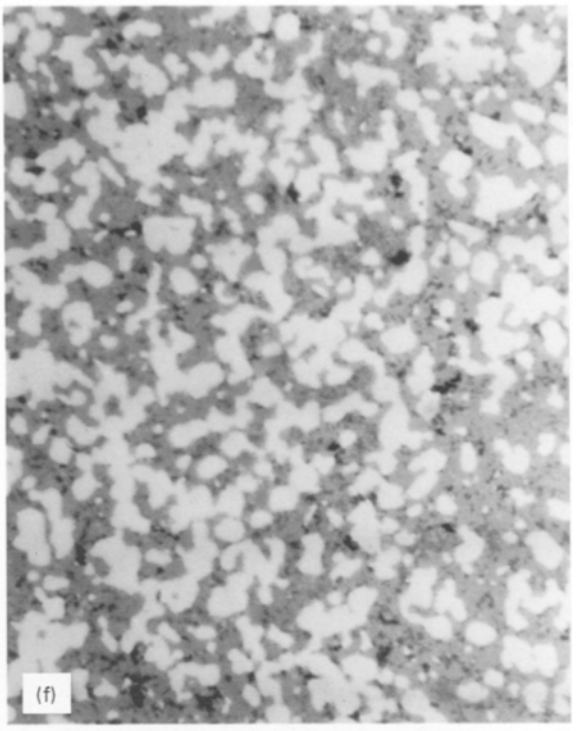

Figure 1 Continued.

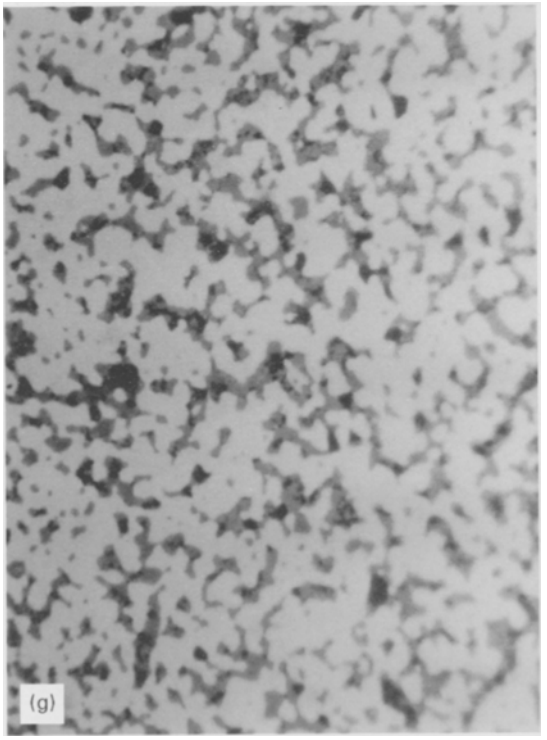

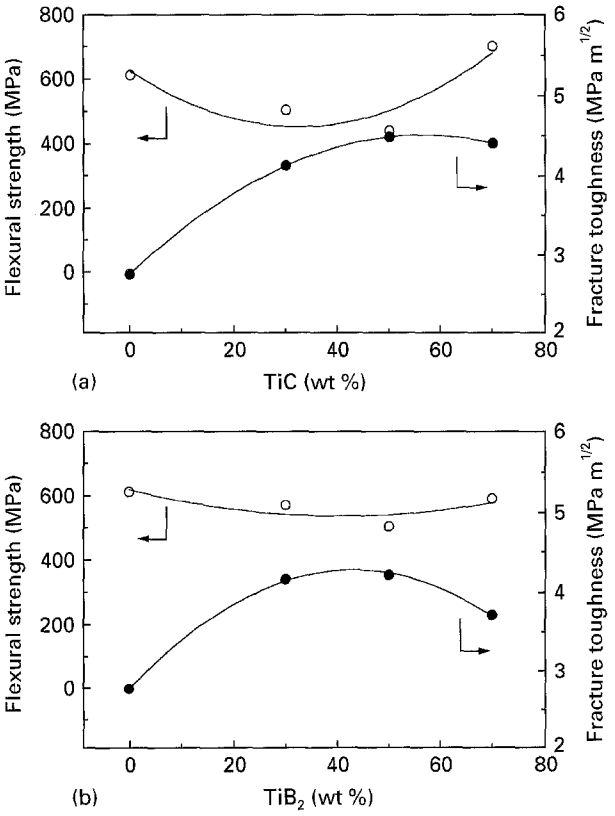

Figure 2 Flexural strength and fracture toughness of (a) SiC–TiC composites, and (b) SiC–TiB_2 composites.

had a fairly planar crack path. Deviations in the crack paths are a result of intergranular fracture in this sample. The amount of crack deflection in SiC–TiC and SiC–TiB_2 composites is larger than that of monolithic SiC. Hence, the increased toughness of SiC–TiC and SiC–TiB_2 composites compared with monolithic SiC, is mainly due to the increased crack deflection around the reinforcing particles.

Another mechanism which may contribute significantly to the observed enhancement of fracture toughness involves stress-induced microcracking of either the particles or the matrix in the immediate vicinity of the particles [21]. Even if the microcracks do not form spontaneously during cooling, the residual tensile stresses in the vicinity of the particles, when added to the stress field of the main crack, may cause microcracking during the crack advance. The decreased strength of SiC–TiC and SiC–TiB_2 composites would be partly due to the residual tensile stress and/or microcracking. Clustering of reinforcing particles,

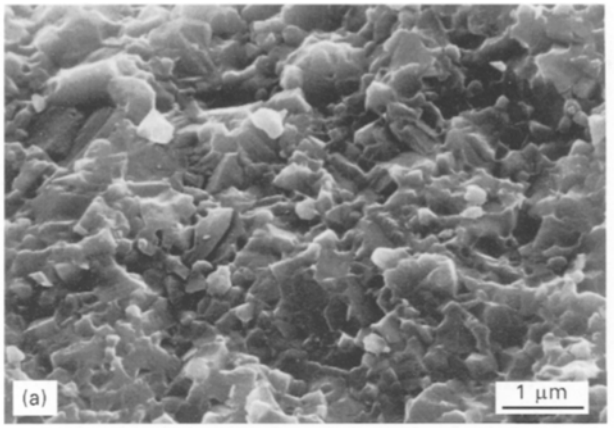

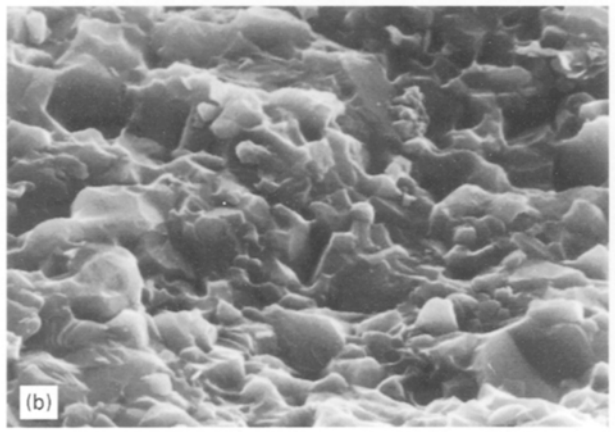

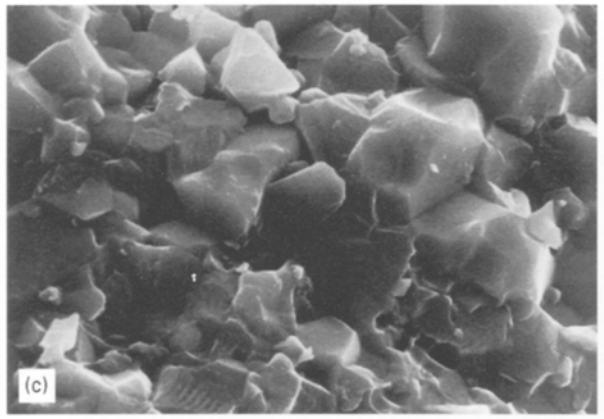

Figure 3 Scanning electron micrographs of fracture surfaces of (a) monolithic SiC, (b) SiC–50 wt % TiC, and (c) SiC–50 wt % TiB_2 composites.

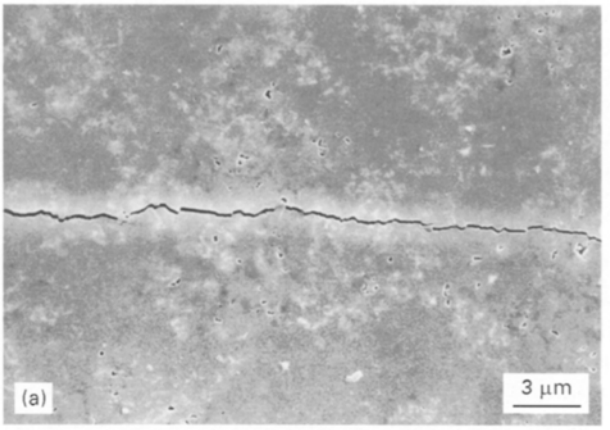

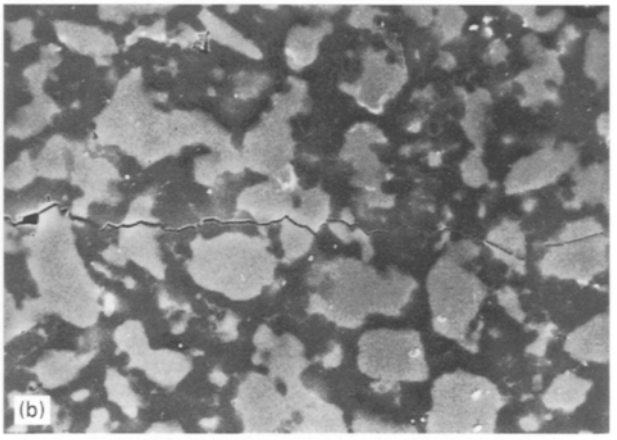

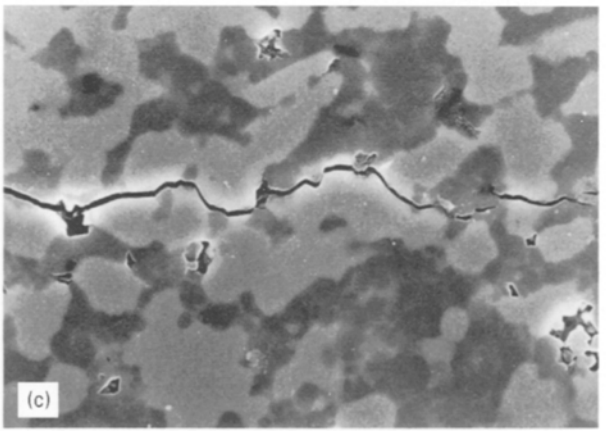

Figure 4 Scanning electron micrographs of a crack path induced by a Vickers' indentor in (a) monolithic SiC, (b) SiC–50 wt % TiC, and (c) SiC–50 wt % TiB_2 composites.

TABLE II Properties of components used to calculate residual stresses

Property	SiC	TiC	TiB_2
Linear thermal expansion coefficient ($°C^{-1}$)	4.16×10^{-6}	7.4×10^{-6}	8.65×10^{-6}
Elastic modulus (GPa)	410	680	531
Poisson's ratio	0.17	0.25	0.25
Electrical resistivity (Ω cm)	$0–10^{+12}$	5.3×10^{-5}	2.8×10^{-5}

which increases the effective critical flaw size of the composites, may also contribute to the observed decrease in strength.

The measured electrical resistivities of monolithic SiC, SiC–TiC and SiC–TiB_2 composites are summarized in Table I. SiC is inherently a semiconductor, and TiC and TiB_2 are inherently good conductors. The SiC–TiC and SiC–TiB_2 composites had electrical resistivities in between SiC and TiC or TiB_2, as expected. A material with a resistivity of $< 1\ \Omega$ cm could

be electrical discharge machined [11]. However, for good machinability, a resistivity $<10^{-2}\,\Omega\,cm$ is required. Our results show that SiC–TiC and SiC–TiB_2 composites, which were investigated in this study, could be electrical discharge machined with good machinability.

4. Conclusion

Dense SiC composites containing 30, 50 and 70 wt % TiC or TiB_2 were fabricated at 1850 °C by hot-pressing with Al_2O_3 and Y_2O_3 as sintering additives. Addition of TiC or TiB_2 particles to SiC matrix increased the toughness and decreased the electrical resistivity, which makes the electrical discharge machining of the composites possible.

Microstructural analysis showed that the toughening was due to the crack deflection, with some possible contribution from microcracking in the vicinity of the reinforcing particles.

References

1. T. T. SHIH and J. OPOKU, *Eng. Fract. Mech.* **12** (1979) 478.
2. J. J. BURKE, E. N. LENOE and R. N. KATZ (eds), "Ceramics for High Performance Applications II" (Brook Hill, Chestnut Hill, MA, 1977).
3. D. J. GODFREY, *Proc. Br. Ceram. Soc.* **22** (1973) 387.
4. A. GHOSH, M. G. JENKINS, K. W. WHITE, A. S. KOBAYASHI and R. C. BRADT, *J. Am. Ceram. Soc.* **72** (1989) 242.
5. Y. W. KIM and J. G. LEE, *J. Mater. Sci.* **27** (1992) 4746.
6. N. P. PADTURE, *J. Am. Ceram. Soc.* **77** (1994) 519.
7. V. D. KRSTIC, *Mater. Res. Soc. Bull.* **20** (1995) 46.
8. M. A. JANNEY, *Am. Ceram. Soc. Bull.* **66** (1987) 322.
9. *Idem, ibid.* **65** (1986) 357.
10. Y. OHYA, M. J. HOFFMAN and G. PETZOW, *J. Am. Ceram. Soc.* **75** (1992) 2479.
11. C. MARTIN, B. CALES, P. VIVIER and P. MATHIEU, *Mater. Sci. Eng.* **A109** (1989) 351.
12. M. RAMULU and M. TAYA, *J. Mater. Sci.* **24** (1989) 1103.
13. K. OKANO, *Ceram. Jpn.* **25** (1990) 195.
14. K. CHIKAMORI, *Kikai Gijutsu Kenkyusho Shoho* **45** (1991) 249.
15. B. R. LAWN and E. R. FULLER, *J. Mater. Sci.* **12** (1975) 2016.
16. Y. W. KIM, H. TANAKA, M. MITOMO and S. OTANI, *J. Ceram. Soc. Jpn.* **103** (1995) 257.
17. M. A. MULLA and V. D. KRSTIC, *Am. Ceram. Soc. Bull.* **70** (1991) 439.
18. D. B. MIRACLE and H. A. LIPSITT, *J. Am. Ceram. Soc.* **66** (1983) 592.
19. S. BAIK and P. F. BECHER, *ibid.* **70** (1987) 527.
20. A. G. EVANCE and T. G. LANGDON, *Prog. Mater. Sci.* **21** (1976) 171.
21. T. I. MAH, M. G. MENDIRATTA and H. A. LIPSITT, *Am. Ceram. Soc. Bull.* **60** (1981) 1229.

Received 10 August 1995
and accepted 2 July 1996